Geostrophic turbulence and the formation of large scale structure

Edgar Knobloch

University of California, Berkeley, CA 94720, USA

knobloch@berkeley.edu

http://tardis.berkeley.edu

Ian Grooms, Keith Julien, Antonio Rubio, Geoff Vasil and Jeff Weiss

IPAM, 31 October 2014

Motivation: Balanced flows (hydrostatic)

- Rotational constraint

$$Ro = \frac{U}{f_0 L} \ll 1$$

- Stable stratification

$$Fr = \frac{U}{NL} \ll 1$$

- Wide aspect ratios

$$\frac{H}{L} \ll 1$$

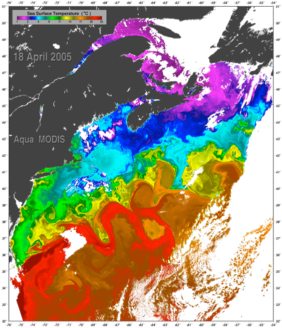

Modis image of Gulf Stream, SST 4/18/2005, NASA.

Observations inform mathematical approximations (QG).

Motivation: Balanced flows (nonhydrostatic)

- Rotational constraint

$$Ro = \frac{U}{f_0 L} \ll 1$$

- Weak stratification

$$Fr = \frac{U}{NL} = \mathcal{O}(1)$$

- Columnar flows

$$\frac{H}{L} > 1$$

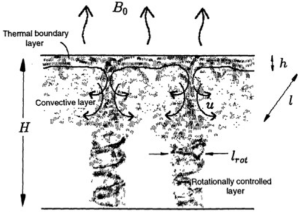

FIG. 1. A schematic representation of the "violent mixing" phase. A homogeneous ocean of depth H, exposed to surface negative buoyancy forcing B_0, responds through the development of a thermal boundary layer of depth h. From this layer intrusions of dense fluid—plumes—penetrate into the quiescent waters beneath having a characteristic length scale l and velocity scale u. These convective circulations sweep fluid out of the boundary layer to depth (and draw fluid up to the surface to be cooled) driving the convection layer below. If the ocean is sufficiently deep (as drawn here) then the convection layer will come under rotational control on the scale $l_{rot} = (B_0/f^3)^{1/2}$.

Jones and Marshall (JPO 1993)

Observations inform mathematical approximations (NHBGE).

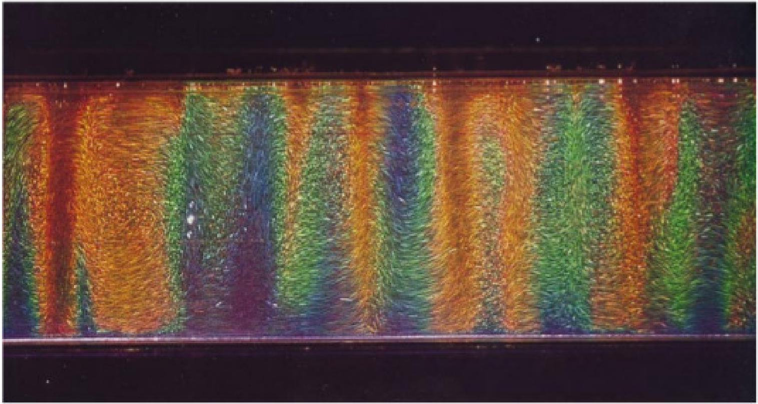

Rotating convection with $H = 6\text{cm}$, $T = 2.6^{\text{deg}}\text{C}$, $\Omega = 14.3\text{rpm}$. From Sakai JFM **333**, 85 (1997)

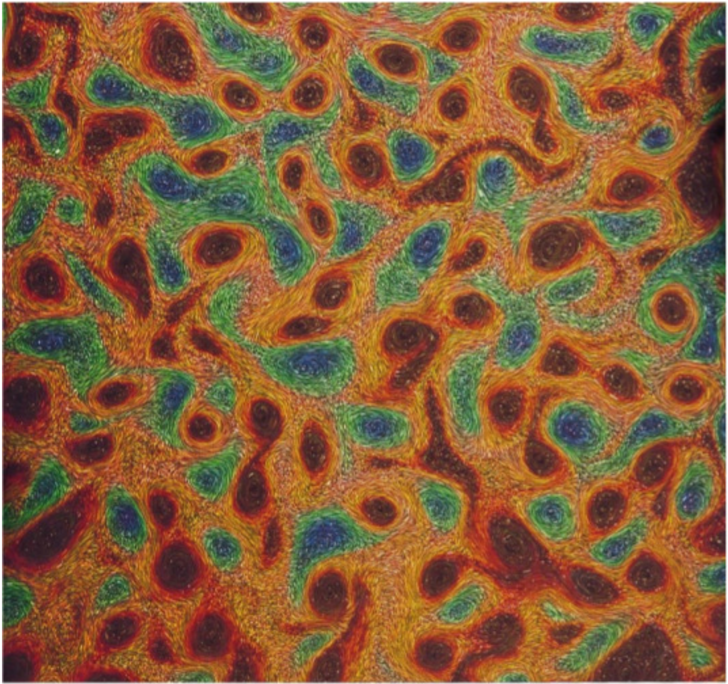

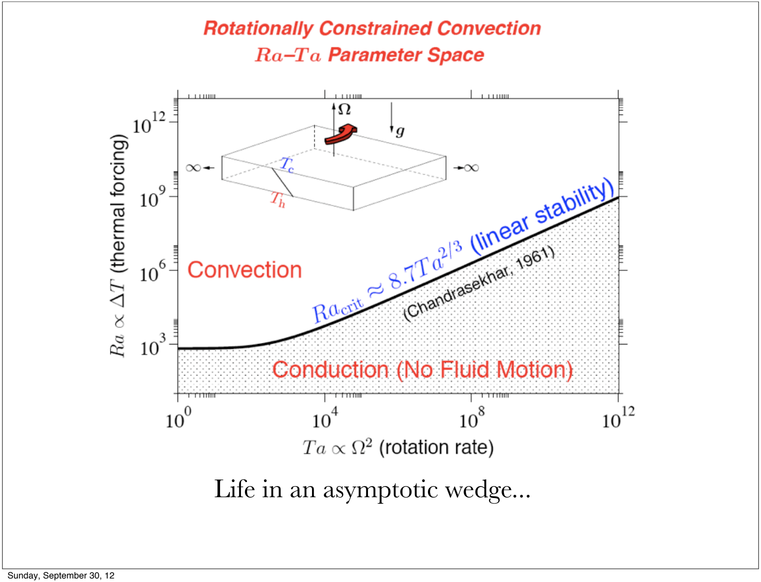

Rotationally Constrained Convection

Ra–Ta Parameter Space

Life in an asymptotic wedge...

Sunday, September 30, 12

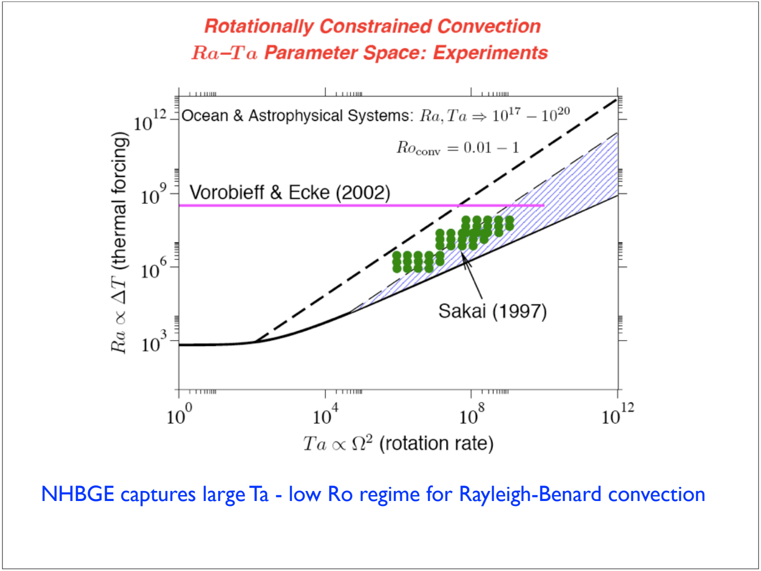

Rotationally Constrained Convection
Ra–Ta Parameter Space: Experiments

NHBGE captures large Ta - low Ro regime for Rayleigh-Benard convection

Sunday, September 30, 12

Basic equations

$$D_t\mathbf{u} + \frac{1}{Ro}\hat{\mathbf{z}} \times \mathbf{u} = -P\nabla p - \Gamma T\hat{\mathbf{z}} + \frac{1}{Re}\nabla^2\mathbf{u}$$

$$D_t T = \frac{1}{Pe}\nabla^2 T$$

$$\nabla \cdot \mathbf{u} = 0,$$

where

$$Ro = \frac{U}{2\Omega L}, \quad P = \frac{\tilde{P}}{\rho_0 U^2}, \quad Re = \frac{UL}{\nu}, \quad Pe = \frac{UL}{\kappa}, \quad \Gamma = \frac{g\alpha\tilde{T}L}{U^2}$$

and L and U are arbitrary horizontal length and velocity scales to be selected depending on the process of interest. We suppose that $Ro \equiv \epsilon \ll 1$ and $H/L = \epsilon^{-1}$ with

$$\partial_t \to \epsilon^{-2}\partial_t + \partial_\tau, \quad \partial_x \to \epsilon^{-1}\partial_x, \quad \partial_y \to \epsilon^{-1}\partial_y, \quad \partial_z \to \epsilon^{-1}\partial_z + \partial_Z.$$

The slow spatial scale Z is required by the boundary conditions.

Asymptotics

An asymptotic expansion in ϵ with $u \sim v \sim W = \mathcal{O}(1)$, and $T = \overline{T} + \epsilon\theta$ leads at $\mathcal{O}(\epsilon^{-1})$ to **geostrophic balance**:

$$\hat{\mathbf{z}} \times \mathbf{u}_\perp = -\nabla_\perp p, \quad \nabla_\perp \cdot \mathbf{u}_\perp = 0, \quad \mathbf{u}_\perp = (-\psi_y, \psi_x), \quad \psi \equiv p$$

At $\mathcal{O}(1)$ the vertical vorticity $\omega \equiv \nabla_\perp^2 \psi$ and vertical velocity W satisfy

$$\partial_t \omega + J[\psi, \omega] - \partial_Z W = Re^{-1} \nabla_\perp^2 \omega$$

$$\partial_t W + J[\psi, W] + \partial_Z \psi = \Gamma\theta + Re^{-1} \nabla_\perp^2 W$$

Fluctuating buoyancy equation at $\mathcal{O}(\epsilon^1)$:

$$\partial_t \theta + J[\psi, \theta] + W \partial_Z \overline{T} = Pe^{-1} \nabla_\perp^2 \theta$$

Mean buoyancy equation at $\mathcal{O}(\epsilon^1)$:

$$\partial_\tau \overline{T} + \partial_Z \overline{W\theta} = Pe^{-1} \partial_{ZZ} \overline{T}.$$

Asymptotics

These equations constitute a **closed reduced system** of equations referred to as NHBGE. In these equations the overbar denotes horizontal average, followed by an average over fast time, and $J(f,g) \equiv f_x g_y - f_y g_x$. The boundary conditions are

$$w = \psi_Z = \theta = 0, \quad \overline{T} = 1, \quad \text{on} \quad Z = 0,$$

$$w = \psi_Z = \theta = 0, \quad \overline{T} = 0, \quad \text{on} \quad Z = 1$$

corresponding to stress-free boundaries. The resulting inviscid dispersion relation for modes of the form $\propto \exp i(\lambda t + \mathbf{k}_\perp \cdot \mathbf{x}_\perp + k_z z)$ is

$$\lambda^2_{\text{reduced}} = \frac{k_z^2}{k_\perp^2}, \qquad \text{cf.} \quad \lambda^2_{\text{NS}} = \frac{k_z^2}{k_\perp^2 + E^{2/3} k_z^2}$$

Thus fast inertial waves on $O(E^{1/3}H)$ vertical scales are filtered out.
Remark: With the choice $L/H = E^{1/3}$ corresponding to the preferred linear theory scale at large rotation rates the expansion parameter is $\epsilon = E^{1/3}$. Here $E \equiv \nu/2\Omega H^2$ is the Ekman number.

Regimes described by the reduced system

The reduced equations describe four distinct dynamical regimes, depending on the values of the Rayleigh number $Ra \equiv g\alpha\Delta TH^3/\nu\kappa$ and the Prandtl number $\sigma \equiv \nu/\kappa$.

- Cellular convection (C)
- Convective Taylor columns (T)
- Convective plumes (P)
- Geostrophic turbulence (G)

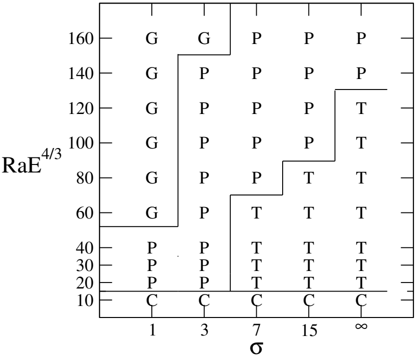

$RaE^{4/3}$ \ σ	1	3	7	15	∞
160	G	G	P	P	P
140	G	P	P	P	P
120	G	P	P	P	T
100	G	P	P	P	T
80	G	P	P	T	T
60	G	P	T	T	T
40	P	P	T	T	T
30	P	P	T	T	T
20	P	P	T	T	T
10	C	C	C	C	C

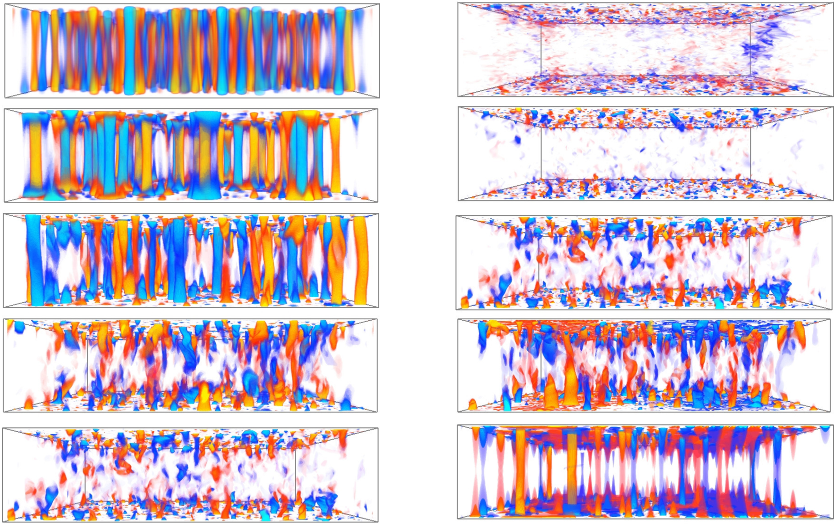

Volume renders of θ for $RaE^{4/3} = 20, 40, 80, 120, 160$ and $\sigma = 7$ (left) and $RaE^{4/3} = 160$ and $\sigma = 1, 3, 7, 15, \infty$ (right)

Geostrophic turbulence

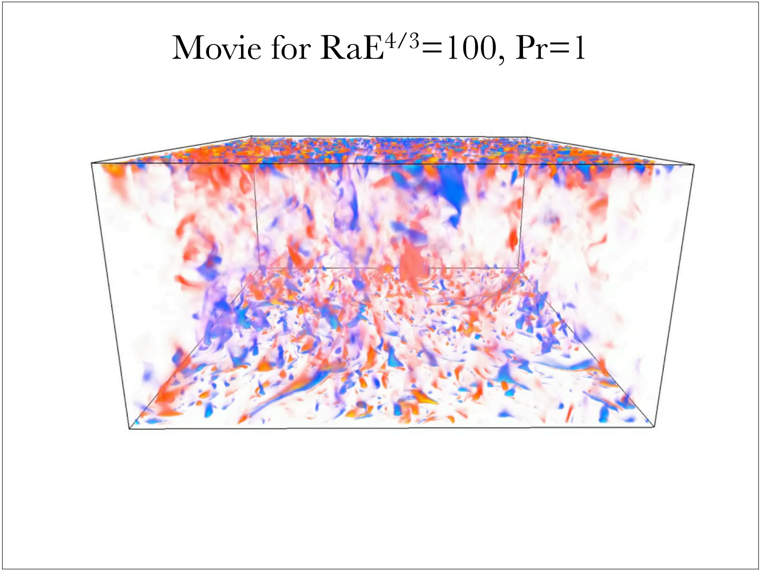

Movie for $RaE^{4/3}=100$, $Pr=1$

Sunday, September 30, 12

Geostrophic turbulence

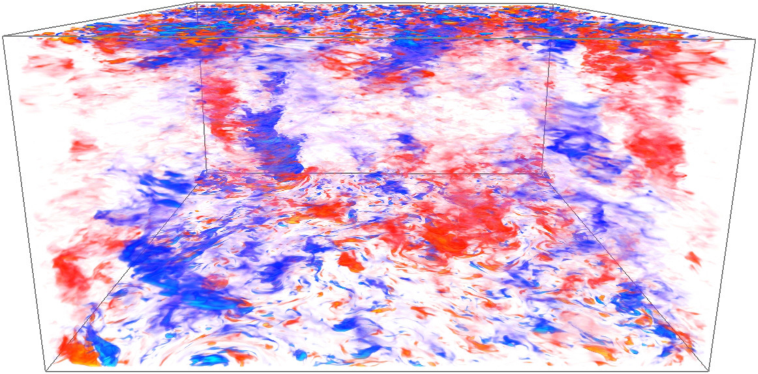

Volume render of θ for $RaE^{4/3} = 160$ and $\sigma = 0.3$

An exact result

The reduced system saturates in a statistically steady state with

$$\overline{W\theta}\,\partial_Z\overline{T} = -\frac{1}{\sigma}\overline{|\nabla_\perp\theta|^2}$$

$$\partial_Z\overline{T} = \sigma\overline{W\theta} - Nu,$$

where Nu is the Nusselt number. Thus

$$\partial_Z\overline{T} = -\frac{1}{2}Nu \pm \frac{1}{2}\left[Nu^2 - 4\overline{|\nabla_\perp\theta|^2}\right]^{1/2}.$$

Thus the thermal dissipation rate is bounded: $\overline{|\nabla_\perp\theta|^2} \leq Nu^2/4$. Since the $-$ sign refers to the thermal boundary layer and the $+$ sign to the bulk the transition between these two regions occurs where $\overline{|\nabla_\perp\theta|^2} = Nu^2/4$. At this location, hereafter $Z = \delta_\epsilon$, we have equipartition between conduction and convection: $-\partial_Z\overline{T} = \sigma\overline{W\theta} = Nu/2$.

Remark: In nonrotating RB convection we have instead

$$\overline{W\theta}\,\partial_Z\overline{T} + \frac{1}{2}\partial_Z\overline{W\theta^2} = -\frac{1}{\sigma}\overline{|\nabla_\perp\theta|^2} - \frac{1}{\sigma}\overline{(\partial_Z\theta)^2}$$

and this relation is not closed.

Boundary layer instability

We use the rescaled equations to analyze the stability of the mean thermal profile as determined from a nonlinear two-point eigenvalue problem for the Nusselt number *Nu* given *R*, and look for the onset of convective instability in the boundary layer.

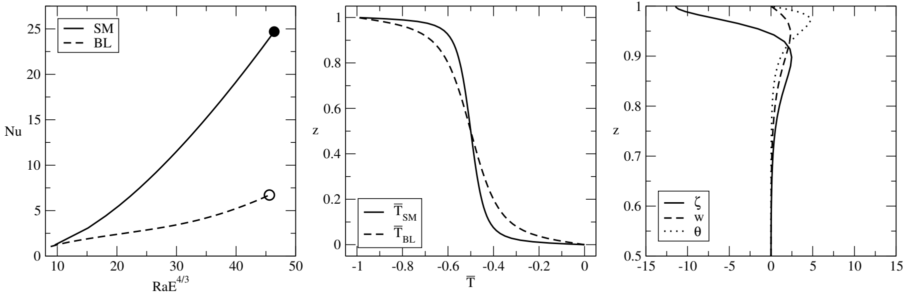

In contrast to RB convection the boundary layer becomes convectively unstable already at small supercriticality.

Boundary layer structure in geostrophic turbulence

We postulate a scaling relation for the structure of the boundary layer of the form

$$\tau = R^{\widehat{\tau}}\, t, \quad \eta = R^{\widehat{\eta}}\, Z, \quad \lambda = R^{\widehat{\lambda}}\, \mathbf{x}_\perp, \quad \psi = R^{\widehat{\psi}}\, \Psi,$$

$$\omega = R^{\widehat{\psi}+2\widehat{\lambda}}\, \Omega, \quad w = R^{\widehat{w}}\, W, \quad \theta = R^{\widehat{\theta}}\, \Theta, \quad \partial_Z \overline{T} = R^{\widehat{\eta}-\Delta} \partial_\eta \overline{T}_\epsilon,$$

where $R \equiv RaE^{4/3} \gg R_c$. Our simulations indicate that all terms remain in play as R increases, leading to the relations

$$\widehat{\lambda} = \widehat{w} = s, \quad \widehat{\eta} = 3s, \quad \widehat{\tau} = \widehat{\Omega} = 2s, \quad \Delta = 1 - s, \quad \widehat{\psi} = 0, \quad \widehat{\theta} = 3s - 1,$$

where $s > 0$. Thus $\mathbf{Nu} \sim \mathbf{R^{4s-1}}$ and we have a one parameter family of scaling solutions.

Comparison with the measured turbulent scaling law $Nu \sim R^{3/2}$ implies that $s = 5/8$ and yields predictions of all other quantities.

Measured turbulent scaling law: $Nu \sim \sigma^{-1/2} R^{3/2}$

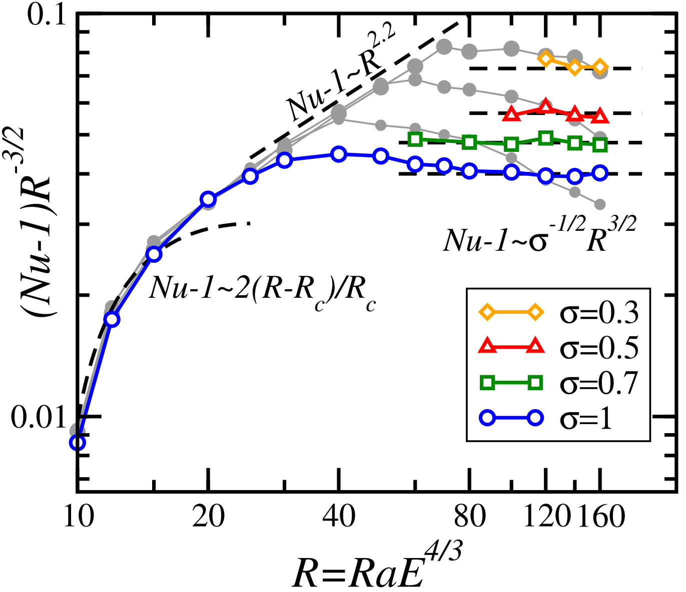

Theoretical interpretation

We postulate a relation of the form

$$Nu - 1 \sim C(\sigma) Ra^{\alpha} E^{\beta}$$

valid for $Ra \gg Ra_c$. In nonrotating convection $0.28 \lesssim \alpha \lesssim 0.31$ (Grossmann and Lohse (2000), Xu et al (2000), Ahlers and Xu (2001)) unless the boundary layers become turbulent when $\alpha \approx 0.38$. Here the mean temperature gradient at midheight decreases to zero as Ra increases. Thus heat transport is limited by the efficiency of the boundary layers.
In rapidly rotating convection the mean temperature gradient at midheight **saturates** as Ra increases and heat transport is limited by the efficiency of the turbulent interior.
For $Ra_c \ll Ra \lesssim Ra_t$ we expect Nu to depend only on Ra/Ra_c. Thus $Nu - 1 \propto (RaE^{4/3})^{\alpha}$. If we suppose that the heat flux is independent of microscopic diffusion coefficients, then $\alpha = 3/2$ ($\beta = 2$), and

$$Nu - 1 \sim C_1 \sigma^{-1/2} Ra^{3/2} E^2$$

with $C_1 \approx 0.04 \pm 0.0025$ from simulations.

Evidence that heat flux in bulk determines *Nu*

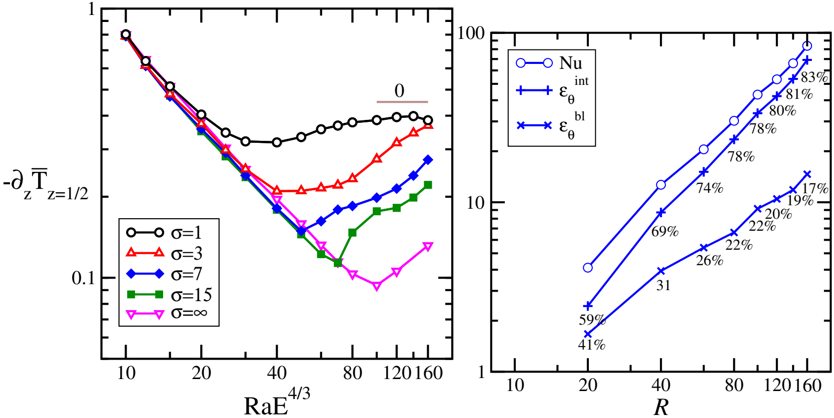

(a) Midheight gradient. (b) Contributions (in percentage form) to $Nu = \langle(\partial_Z \overline{T})^2\rangle + \langle|\nabla_\perp \theta|^2\rangle$ from the bulk ($\mathcal{E}_\theta^{\rm int}$) and the boundary layers ($\mathcal{E}_\theta^{\rm BL}$). Heat transport is limited by the efficiency of the turbulent interior.

Evidence for $s = 5/8$

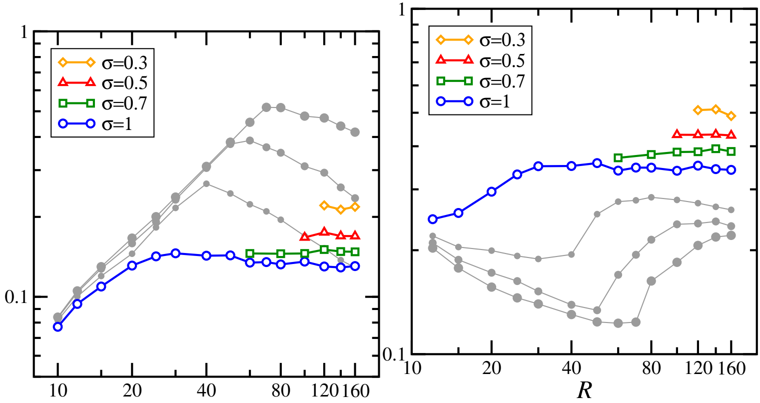

Compensated plots of (a) $\theta E^{-1/3} R^{-7/8}$, (b) $W \sigma E^{1/3} R^{-5/8}$

Evidence for $s = 5/8$

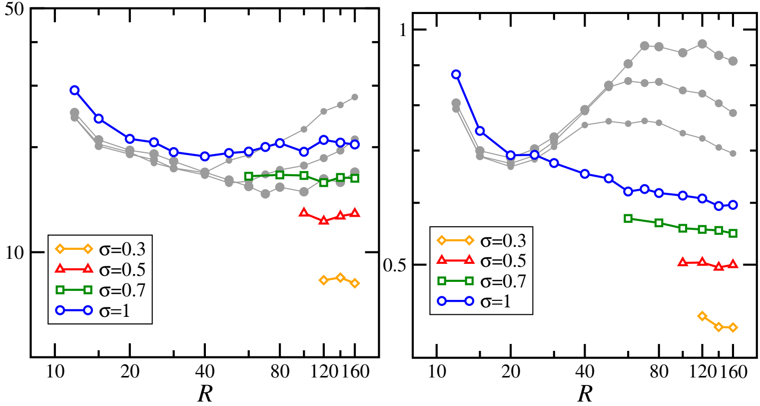

Compensated plots of (a) boundary layer width $\eta R^{15/8}$, (b) associated temperature drop $\delta \overline{T} R^{3/8}$

Transition to nonrotating scaling

As Ra increases at fixed rotation rate we expect a transition to nonrotating scaling. This is a consequence of increasing convective Rossby number $Ro_{\rm conv} \equiv E\sqrt{Ra/\sigma}$.

We conjecture that the transition to nonrotating scaling is triggered by the loss of geostrophic balance in the boundary layer, i.e., when the boundary layer Rossby number $Ro_{\rm loc} \equiv E_{\rm loc} Ra_{\rm loc}^{1/2} \sim 1$. Here $E_{\rm loc} = E\eta^{-2}$ and $Ra_{\rm loc} = Ra(\Delta T_{\rm loc}/\Delta T)\eta^3 = Ra\, Nu\, \eta^4$, where $\eta \sim R^{-3s} H$ is the boundary layer width. Since $Nu \sim R^{4s-1}$ and $Ra = R\, E^{-4/3}$, it follows that $E_{\rm loc} = E\, R^{6s} \equiv \varepsilon^3$ and $Ra_{\rm loc} = E^{-4/3} R^{-8s} \equiv \varepsilon^{-4}$, where $\varepsilon \equiv E^{1/3} R^{2s}$. It follows that $Ro_{\rm loc} \sim \varepsilon$ and hence that $Ro_{\rm loc} \sim 1$ when $E^{1/3} R^{2s} \sim 1$. Since $s = 5/8$ this occurs when Ra reaches $Ra_t \sim E^{-8/5}$, or equivalently when $Ro = Ro_t \sim E^{1/5}$. Since $E \ll 1$ the transition Rossby number $Ro_t \ll 1$, i.e., the transition from the 3/2 scaling law occurs in the rapidly rotating regime.

There is some evidence for the validity of these predictions as shown next.

Nusselt number scaling (from King et al 2012)

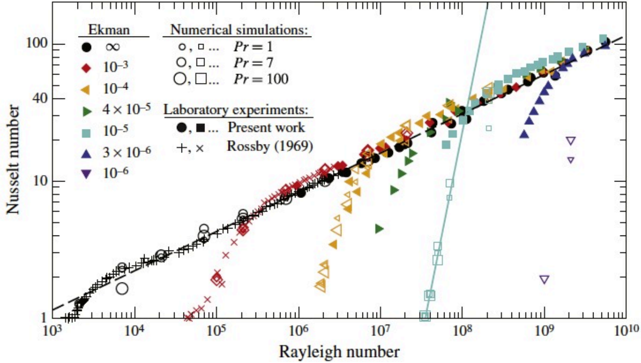

$Ro_t \to 0$ as $E \to 0$

King et al NATURE (2009)
and King et al JFM (2012)

Sunday, September 30, 12

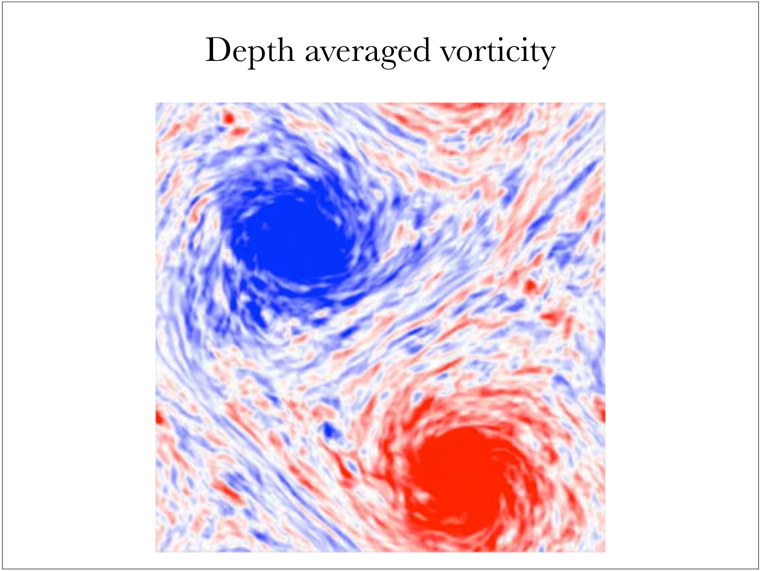

Depth averaged vorticity

Sunday, September 30, 12

Julien et al, GAFD **106**, 392–428 (2012)

Julien et al, GAFD **106**, 392–428 (2012)

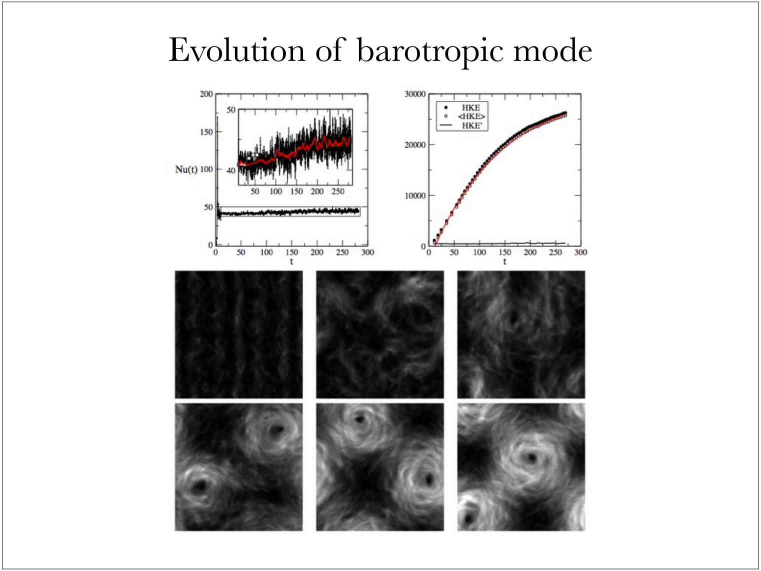

Evolution of barotropic mode

Sunday, September 30, 12

Julien et al, GAFD **106**, 392–428 (2012)

Spontaneous formation of large scale vortices

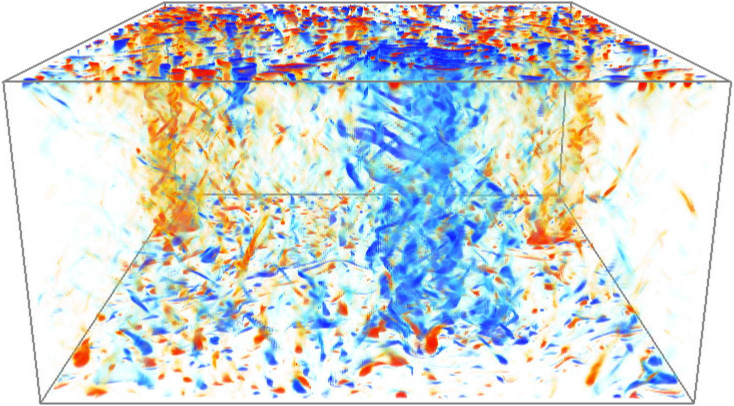

Rubio et al, PRL **112**, 144501 (2014)

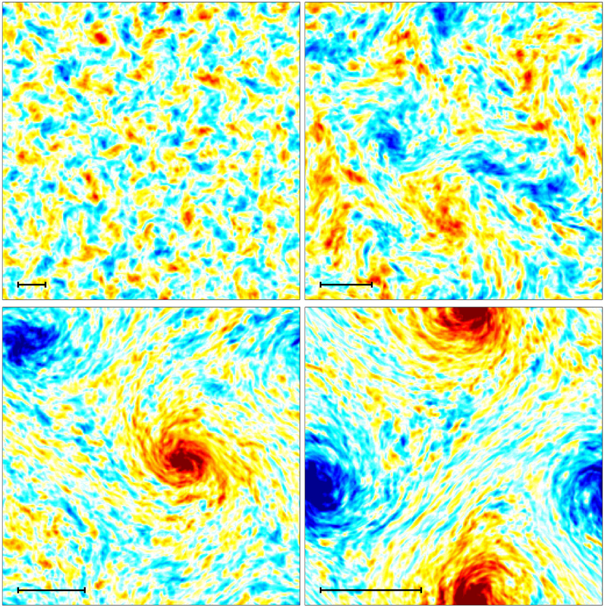

(a) $t = 1$, (b) $t = 10$, (c) $t = 37.5$, (d) $t = 100$

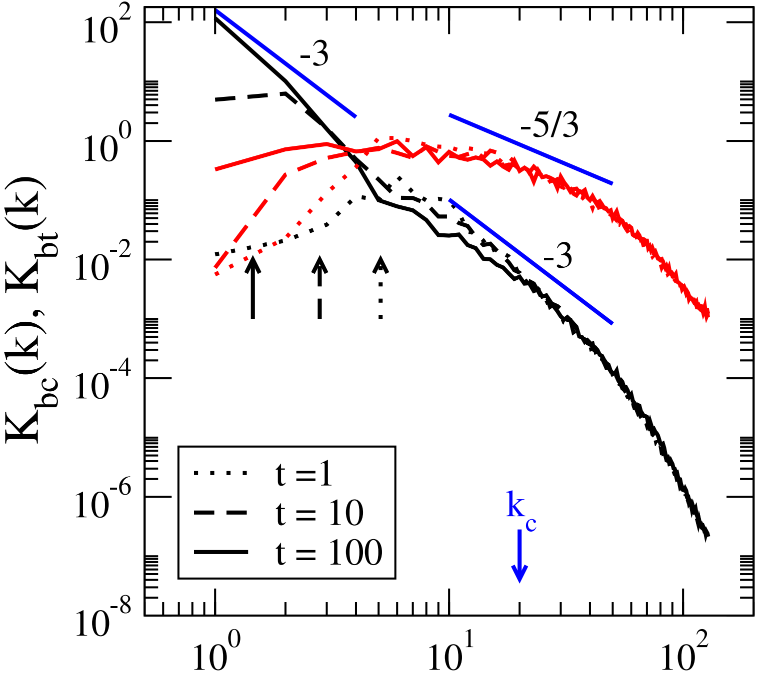
$K_{bc}(k), K_{bt}(k)$
10^2
10^0
10^{-2}
10^{-4}
10^{-6}
10^{-8}
10^0
10^1
10^2
-3
-5/3
-3
k_c
t =1
t = 10
t = 100

Barotropic/baroclinic vorticity equations

Let $\omega = \langle\omega\rangle + \omega'$, $\psi = \langle\psi\rangle + \psi'$, where $\langle\dots\rangle$ denotes a depth average.

Then

$$\langle\omega\rangle_t + J[\langle\psi\rangle, \langle\omega\rangle] + \langle J[\psi', \omega']\rangle = \nabla_\perp^2\langle\omega\rangle$$

and

$$\omega'_t + J[\langle\psi\rangle, \omega'] + J[\psi', \langle\omega\rangle] + J[\psi', \omega']' - DW = \nabla_\perp^2\omega'$$

Thus the baroclinic-baroclinic term acts as a source term for the barotropic mode. Without this term the barotropic flow is identical to 2D hydrodynamics and an inverse energy cascade to large scales is expected. In fact this is so even in the presence of this term, and leads to a $k_\perp^{-3}$ pile up at large scales, eg., Smith and Waleffe, Phys. Fluids **11**, 1608 (1999).

However, the fluctuation equation is fully 3D and hence exhibits the usual $k_\perp^{-5/3}$ energy spectrum expected from Kolmogorov theory.

The emergence of a coherent structure from a turbulent state has been termed spectral **condensation** (PRL **95**, 263901 (2005); **101**, 194504 (2008); **112**, 144501 (2014)).

Formation of large scale vortices: spectral description

The growth of barotropic kinetic energy at horizontal wave number **k** obeys

$$\partial_t K_{bt}(\mathbf{k}) = T_{\mathbf{k}} + F_{\mathbf{k}} + D_{\mathbf{k}},$$

where $T_{\mathbf{k}} \equiv \sum_{\mathbf{pq}} T_{\mathbf{kpq}}$ and $F_{\mathbf{k}} \equiv \sum_{\mathbf{pq}} F_{\mathbf{kpq}}$ represent, respectively, the symmetrized transfer of energy between Fourier modes within the barotropic component and the transfer of energy between baroclinic and barotropic modes; $D_{\mathbf{k}} \equiv -k^2 K_{bt}$ is the viscous dissipation of the barotropic mode. Moreover,

$$\begin{aligned} T_{\mathbf{kpq}} &= b_{\mathbf{pq}} \mathrm{Re}\left[\langle\psi_{\mathbf{k}}\rangle\langle\psi_{\mathbf{p}}\rangle\langle\psi_{\mathbf{q}}\rangle\right]\delta_{\mathbf{k}+\mathbf{p}+\mathbf{q},\mathbf{0}}, \\ F_{\mathbf{kpq}} &= b_{\mathbf{pq}} \mathrm{Re}\left[\langle\psi_{\mathbf{k}}\rangle\langle\psi'_{\mathbf{p}}\psi'_{\mathbf{q}}\rangle\right]\delta_{\mathbf{k}+\mathbf{p}+\mathbf{q},\mathbf{0}}, \\ b_{\mathbf{pq}} = b_{\mathbf{qp}} &\equiv \frac{1}{2}(p^2 - q^2)(p_x q_y - p_y q_x). \end{aligned}$$

These transfer rates can be computed from the simulations.

Time evolution of baroclinic and barotropic modes

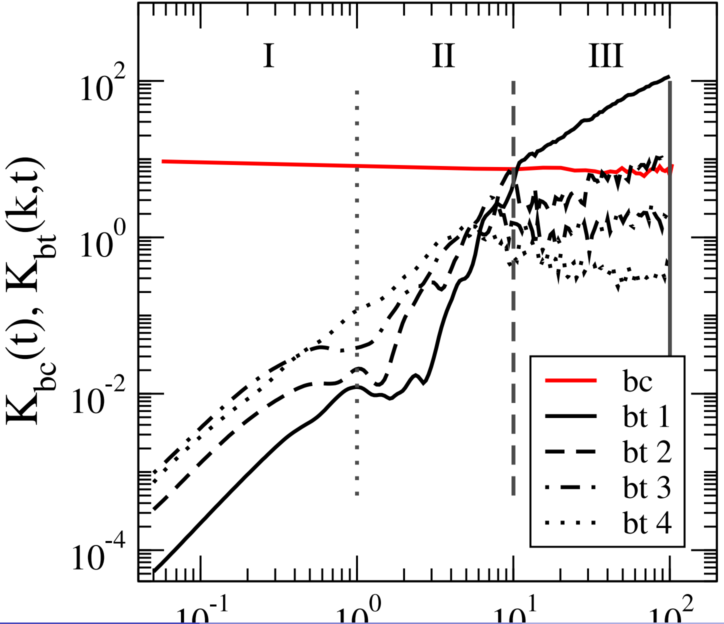

Transfer rates $T_\mathbf{k}$ and $F_\mathbf{k}$ at three successive times

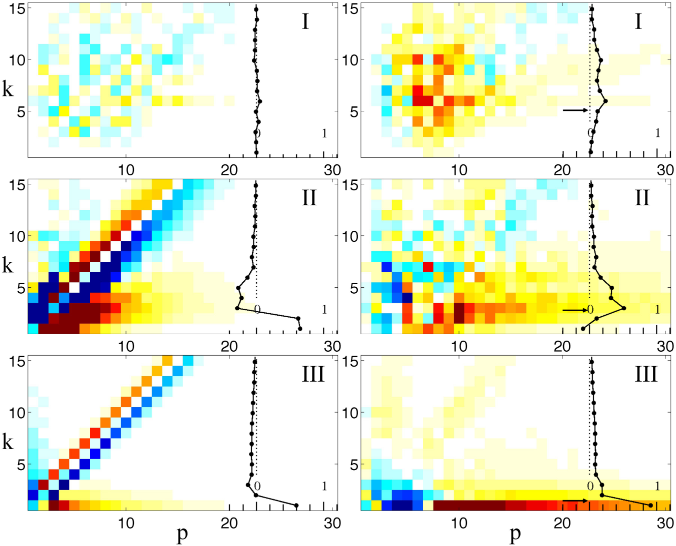

Unreasonable effectiveness of asymptotics ($E = 10^{-7}$)

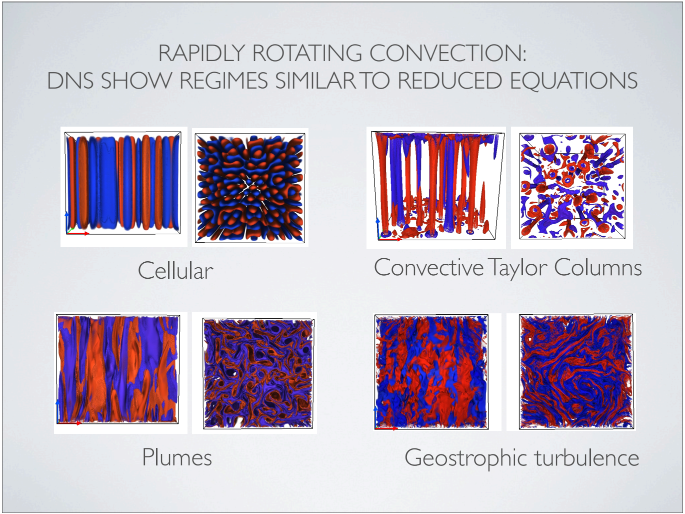

RAPIDLY ROTATING CONVECTION:
DNS SHOW REGIMES SIMILAR TO REDUCED EQUATIONS

Cellular

Convective Taylor Columns

Plumes

Geostrophic turbulence

Cellular regime: $Pr = 1$, $E^{4/3}Ra = 11$; CTC Regime: $Pr = 15$, $E^{4/3}Ra = 15$; Plume Regime: $Pr = 3$, $E^{4/3}Ra = 50$; GT Regime: $Pr = 1$, $E^{4/3}Ra = 90$

Conclusions

Heat transport in rapidly rotating convection ($E \ll 1$):

- At large Ra the Nusselt number scales as $Nu - 1 \approx C_1 \sigma^{-1/2} Ra^{3/2} E^2$ with $C_1 \approx 0.04 \pm 0.0025$.
- This scaling is a consequence of inefficient heat transport in the turbulent bulk
- This is a result of the saturation of the midheight mean temperature gradient as Ra increases
- The scaling is a consequence of the scaling behavior of the boundary layers at large Ra
- Transition from this scaling occurs when the local Rossby number in the boundary layer becomes of order unity, i.e., at $Ra_t \sim E^{-8/5}$ as $E \rightarrow 0$, or equivalently when $Ro = Ro_t \sim E^{1/5}$.

Geostrophic turbulence in this system is unstable to a large scale barotropic (vortical) mode

- The spectra of the barotropic and baroclinic components of the HKE are consistent with the Kraichnan and Kolmogorov pictures (2D conserves energy and enstrophy, 3D conserves energy only)

Conclusions (ctd)

- Baroclinic-baroclinic forcing injects energy directly to the largest scales despite the small scale nature of the baroclinic fields
- Certain aspects of these predictions have been confirmed in simulations of the primitive equations by Stellmach (2012), Favier et al (PF **26**, 096605, 2014) and Guervilly et al (JFM 758, 407, 2014).
- The fact that a fully 3D turbulent flow exhibits a large scale instability may have geophysical and astrophysical implications

References:

K Julien, E Knobloch and J Werne, Th. Comp. Fl. Dyn. **11**, 251–261 (1998)
M Sprague, K Julien, E Knobloch and J Werne, JFM **551**, 141–174 (2006)
K Julien, E Knobloch, R Milliff and J Werne, JFM **555**, 233–274 (2006)
I Grooms, K Julien, J B Weiss and E Knobloch, PRL **104**, 224501 (2010)
K Julien, A M Rubio, I Grooms and E Knobloch, GAFD **106**, 392–428 (2012)
K Julien, E Knobloch, A M Rubio and G M Vasil, PRL **109**, 254503 (2012)
A M Rubio, K Julien, E Knobloch and J B Weiss, PRL **112**, 144501 (2014)